Minimising residual aberration in the presence of cyclotorsion uncertainty in refractive surgery

Samuel Arba-Mosquera, PhD[1,2,3]; Diego de Ortueta, MD[4]; Shwetabh Verma, MSc[1,5,6,7]

PURPOSE: To formulate a simple valid method to minimize the residual aberration magnitudes due to uncertainty in cyclotorsion measurement.

SETTING: Optics research laboratory.

METHODS: Assuming that cyclotorsion error can be estimated and compensated for with a certain level of uncertainty, we formulate a function to modify the wavefront error in order to minimize the residual aberration magnitudes due to cyclotorsion measurement uncertainty. A modal optimum nomogram factor is computed for minimization of the residual aberration for each Zernike mode. We also calculate the optimized residual aberration using the minimization factor.

RESULTS: For modal optimum, the minimization factor was dependent only on Zernike meridional order and cyclotorsion uncertainty. The value of the minimization function ranged between –1 and +1.

CONCLUSION: In a perfectly performing system, an "overplanned" treatment will never minimize residual wavefront aberration, independent of the cyclotorsion uncertainty. An "underplanned" treatment calculated using the presented approach will minimize the residual aberration magnitude imposed by the higher order Zernike terms, and will reduce its relative orientation to the original aberration pattern. The gains using this method are undeniably modest, but at such low implementation costs can still be valuable.

J Emmetropia 2016; 3: 139-144

The optical quality of human eyes is often described in terms of wavefront aberrations. The distribution and contribution of each aberration to the overall wavefront aberration in the individual eye can now be accurately determined and predicted.

Submitted: 2/4/2016
Revised: 11/14/2016
Accepted: 11/29/2016

[1]SCHWIND eye-tech-solutions GmbH, Kleinostheim. Germany.
[2]Recognized Research Group in Optical Diagnostic Techniques, University of Valladolid. Spain.
[3]Department of Ophthalmology and Vision Sciences, University of Oviedo. Spain.
[4]Augenzentrum Recklinghausen, Recklinghausen. Germany.
[5]Experimental Radiation Oncology, University Medical Center Mannheim, Heidelberg University. Germany.
[6]Interdisciplinary Center for Scientific Computing (IWR), Heidelberg University. Germany.
[7]Central Institute for Computer Engineering (ZITI), Heidelberg University. Germany.

Financial Disclosure: This study has been conducted with no external financial support. Shwetabh Verma and Samuel Arba-Mosquera are employees of SCHWIND eye-tech-solutions.

Corresponding Author: Samuel Arba Mosquera
SCHWIND eye-tech-solutions GmbH.
Mainparkstrasse 6-10, D-63801 Kleinostheim, Germany
E-mail: sarbamo@cofis.es

Wavefront measurement techniques and the driven refractive procedures are designed based on the Zernike polynomials[1] and their associated coefficients unique to the patient's wavefront map. The success of wavefront-based refractive surgery procedures relies on accurate measurement of wavefront aberrations and corresponding precise laser-based correction. Correcting the higher order aberration of the eye requires lasers with smaller spots and finer resolution[2], and the growing laser industry is catering well to this need. A top-hat laser beam of 1 mm (Gaussian with FWHM of 0.76 mm) is small enough to produce a customized ablation for typical human eyes[3]. This means, for high accuracy in refractive correction, it is all the more necessary to position the laser spots with very high precision, since reduction of spot diameter has been shown to make the correction more susceptible to eye movement-induced error[4,5].

Several factors may influence the landing of laser pulses on the intended location. Among them are the torsional/rolling movements of the eye. Laser refractive surgery is designed based on the information gathered from the diagnostic tests. In clinical practice, diagnostic tests are usually performed with the patient in an upright position, while the refractive surgery procedure is performed with the patient in a supine

© 2016 SECOIR
Sociedad Española de Cirugía Ocular Implanto-Refractiva

position. This change in the head position produces some rolling of the eye along the visual axis, called static cyclotorsion. In addition to this, dynamic torsional movements also affect refractive procedures; these are the small torsional movements observed while the head is in supine position. Studies have shown, on average, a small amount of cyclotorsion (<2°) and magnitude of dynamic pupil decentration from the laser centre during treatment (277.0 ± 44.07 μm)[6].

Most sophisticated refractive surgery laser systems are now able to track the rolling movement of the eye and rotate the ablation profile with the corresponding torsional angle, compensating for the cyclotorsion movements (or the cyclotorsion error). This measurement, however, is subject to errors due to noise and other factors. The result is imperfect cyclotorsion compensation producing some degree of mismatch in the applied ablation profiles versus the intended ones[7,8]. The extent of this mismatch is dependent on the magnitude of the cyclotorsion error.

It is often misreported that uncompensated cyclotorsion results in undercorrections. Recent studies have shown that, in general, uncompensated cyclotorsion actually results in residual aberrations[9-12]; however, non-rotationally symmetric aberration terms (like astigmatism) are accentuated more than others. Swami et al.[13] measured the rotational position of eyes that underwent treatment for myopic or hyperopic astigmatism, concluding that a 4° and 10° misalignment would theoretically result in a 14% and 35% undercorrection of astigmatism, respectively.

Assuming that the cyclotorsion angle can be estimated and compensated for with a certain level of uncertainty introduced by the components involved in the measurement, we formulate a function to modify the wavefront error in order to minimize the residual aberration magnitudes due to this uncertainty in cyclotorsion measurement. Shi et al.[14] have recently provided an insight on this topic. They developed a stochastic parallel gradient descent (SPGD)-based algorithm to optimize wavefront-guided correction that improves visual acuity given cyclotorsion errors, based on measured scleral contact lens movements for three keratoconous eyes. Their method is iterative, and is based on initially recorded scleral movements. The presented method, however, aims at solving the same problem but with a more general, simple mathematical approach.

METHODS

The Zernike polynomials are neither scale nor translation invariant[15]. On the other hand, for torsional eye movement, invariance of the Zernike coefficients holds due to the independent nature of cyclotorsion effects with the radial order[9,15-17].

Many researchers have explored the transformation of Zernike coefficients under the rotation, translation and scaling movements of the eye. Particular to the rotation movements, each pair of Zernike terms with the same radial order *(n)* and angular frequency *(m)* transforms through a rotation matrix of angle $m\theta$, where θ is the rotation angle[15]. When the rotation angle is 0, the aberration and ablation patterns cancel each other, resulting in no residual aberration. Based on the definition of the Zernike polynomials[15] ($Z(n,m)$, where n is a null or positive integer and m is an integer ranging from $-n$ to $+n$, representing the radial and meridional orders, respectively), it is evident that the polynomials $Z(n,0)$ are invariant under rotations around their center. Therefore, only vectorial aberrations are affected by cyclotorsion errors. For those, Zernike polynomials are structured in two complementary sets, governed by sine/cosine functions that avoid coupling of different orders of aberration for rotations around the center.

After rotation of the opposite Zernike components around their origins, the aberration mode still can be decomposed into two Zernike components[9]:

$$C_n^{'m} = -[C_n^m \cdot \cos(m \cdot \theta) + C_n^{-m} \cdot \sin(m \cdot \theta)] \quad (1)$$

Where n is the radial order; m, the angular frequency; $C_n^{'m}$, the rotated Zernike compensation; C_n^m, the original Zernike components; and θ, the cyclotorsion error. Here, the term cyclotorsion "error" is used to represent the error induced in the ablation due to the cyclotorsion angle of the eye.

After compensating for the original pattern with a rotated one, the residual wavefront error component is given by the equation[9]:

$$R_n^m = C_n^m \cdot [1 - \cos(m \cdot \theta)] - C_n^{-m} \cdot \sin(m \cdot \theta) \quad (2)$$

Where R_n^m is the residual aberration component. The measured cyclotorsion can be accurate (θ) or affected by measurement uncertainty (θ influenced by θ_u, where θ_u is the measurement uncertainty). We assume that the residual aberration can be attributed to either the cyclotorsion error only (θ), or the cyclotorsion error measured in the presence of measurement uncertainty (θ influenced by θ_u). In order to minimize the residual term, we employ two analytical optimization approaches, a) Modal optimization to minimize residual aberrations due to cyclotorsion error (θ), and b) Modal optimization to minimize residual aberrations due to cyclotorsion error in the presence of measurement uncertainty (θ influenced by θ_u). In the former, we modify each Zernike mode to obtain a minimization factor that minimizes the residual aberration due to the cyclotorsion error (θ). In the latter, we modify each Zernike mode to obtain a minimization factor that minimizes the sum of square residual wavefront aberration due to the cyclotorsion errors in the presence of measurement uncertainty (θ and θ_u). Note that the cyclotorsion error (θ) and cyclotorsion measurement uncertainty (θ_u) are deemed as different terms. Furthermore, this approach should be seen as an optimization of the existing techniques of rotating the ablation profiles to compensate for the cyclotorsion errors, rather than an alternative to the same.

a) Modal optimization to minimize residual aberrations due to cyclotorsion error

Let us assume that we have the freedom to adjust the magnitude of each Zernike mode:

$$T_n^{\pm m} = F_n^m \cdot C_n^{\pm m} \quad (3)$$

Where $T_n^{\pm m}$ is the treated aberration component and F_n^m is the minimization factor for each Zernike mode. We use the same minimization factor for the Zernike terms in each mode, governed by the same sine/cosine relationship amongst modes within the same radial order. For the same cyclotorsion error, the residual components would be given by[9]:

$$R_n^m = C_n^m - T_n^m \cdot \cos(m \cdot \theta) - T_n^{-m} \cdot \sin(m \cdot \theta) \quad (4)$$

$$R_n^m = C_n^m \cdot [1 - F_n^m \cdot \cos(m \cdot \theta)] - C_n^{-m} \cdot F_n^m \cdot \sin(m \cdot \theta) \quad (5)$$

Expressing each residual aberration mode in magnitude we get:

$$|R_n^{\pm m}| = \sqrt{(R_n^{-m})^2 + (R_n^{+m})^2} \quad (6)$$

Similarly, each Zernike coefficient mode can be expressed in magnitude as:

$$|C_n^{\pm m}| = \sqrt{(C_n^{-m})^2 + (C_n^{+m})^2} \quad (7)$$

Using Eqs. 4-7, we can express the residual aberration mode in magnitude as:

$$|R_n^{\pm m}| = |C_n^{\pm m}| \cdot \sqrt{(F_n^m)^2 - 2 \cdot F_n^m \cdot \cos(m \cdot \theta) + 1} \quad (8)$$

Calculation of the above expression is based on the assumption that the measured cyclotorsion error is accurate and the resulting magnitude of residual aberrations due to the cyclotorsion error can be minimized by the modal function F_n^m.

The factor that minimises the residual Zernike mode is the minimum of the square root term in Eq. (8); thus the term that minimises the quadratic function inside the square root (the vertex of the parabola) is calculated to be:

$$F_n^m = \cos(m \cdot \theta) \quad (9)$$

In addition, using Eqs. (8) and (9), the residual aberration (considering accurate cyclotorsion measurement) can be calculated as follows:

$$|R_n^{\pm m}| = |C_n^{\pm m}| \cdot \sqrt{(\cos(m \cdot \theta))^2 - 2 \cdot \cos(m \cdot \theta) \cdot \cos(m \cdot \theta) + 1} \quad (10)$$

$$|R_n^{\pm m}| = |C_n^{\pm m}| \cdot \sin(m \cdot \theta) \quad (11)$$

Notice that F_n^m is always between [–1, +1] and that F_n^m changes its sign when $m \cdot \theta = \pi / 2$.

b) Modal optimization to minimize residual aberrations due to cyclotorsion error in the presence of measurement uncertainty

In the event that cyclotorsion error is measured with some uncertainty, we can express the sum of square residuals by modifying Eq. 8 as:

$$(|R_n^{\pm m}|)^2 = (|C_n^{\pm m}|)^2 \cdot \int_{-\theta_u}^{+\theta_u} ((Fu_n^m) - 2\,(Fu_n^m) \cos(m \cdot \theta) + 1)\, d\theta \quad (12)$$

Where θ_u is the uncertainty in measuring the cyclotorsion error and Fu_n^m is the modal factor that minimizes the residual aberration due to the cyclotorsion error in the presence of measurement uncertainty.

A modal minimization factor that minimizes the sum of square residuals can be calculated using Eq. 12 as:

$$Fu_n^m = \frac{\sin(m \cdot \theta_u)}{m \cdot \theta_u} \quad (13)$$

In addition, the residual aberration magnitude using the above minimization function (considering uncertainty in cyclotorsion measurement) can be calculated from Eqs. (13) and (8) as:

$$|R_n^{\pm m}| = |C_n^{\pm m}| \cdot \sqrt{\left(\frac{\sin(m \cdot \theta_u)}{m \cdot \theta_u}\right)^2 - \frac{2 \sin(m \cdot \theta_u) \cos(m \cdot \theta)}{m \cdot \theta_u} + 1} \quad (14)$$

RESULTS

Figure 1 presents the results of the modal optimization method. Notice that the X-axis, being a product of angular frequency and cyclotorsion error/uncertainty, represents the behaviour of the methods for a general range of angular frequencies in combination with a range of cyclotorsion error/uncertainty. We designate the X-axis as a product of angular frequency *(m)* and cyclotorsion error in Figure 1A, and as a product of angular frequency *(m)* and cyclotorsion uncertainty in Figure 1B to differentiate the methods using accurate cyclotorsion error and cyclotorsion error in the presence of measurement uncertainty, respectively. The Y-axis represents the residual aberration expressed in percentage, calculated with or without the corresponding optimization factor. Although cyclotorsion error/uncertainty beyond 20° is very implausible, a higher range is used in the X axis for demonstrative purposes, for both higher Zernike orders and cyclotorsion error/uncertainty.

a) Modal optimization to minimize residual aberrations due to cyclotorsion error

This method is presented in Figure 1A, with the residual aberrations calculated without (residual aberration using Eq. 2) and with the effect of modal optimization factor (minimized residual using Eq. 10), expressed in percentage.

b) Modal optimization to minimize residual aberrations due to cyclotorsion error in the presence of measurement uncertainty

This method is presented in Figure 1B, with the residual aberrations calculated without (residual aberration using Eq. 2) and with the effect of modal optimization factor (minimized residual using Eq. 14), expressed in percentage.

A limitation of the obtained optimization factors is that they are based on an initially estimated cyclotorsion error, which is assumed to be either accurate or affected

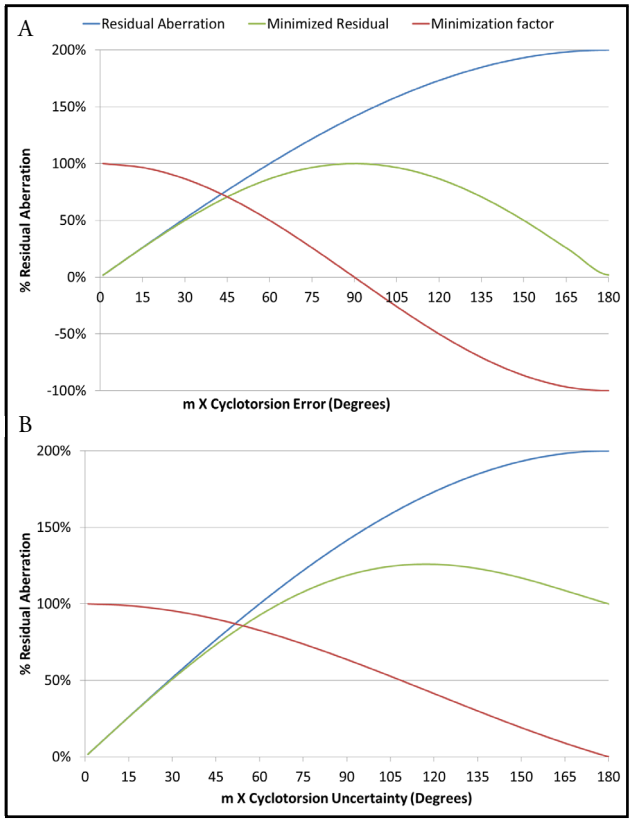

Figure 1. Behaviour of the minimization factor and non-optimized and optimized residual aberration with increasing cyclotorsion error/uncertainty. (a) Using modal optimization based on accurate cyclotorsion error. (b) Using modal optimization based on cyclotorsion error in the presence of measurement uncertainty. The X-axis being a product of angular frequency and cyclotorsion error/uncertainty represents the behaviour of the methods for a range of angular frequencies in combination with a range of cyclotorsion error/uncertainty. The Y-axis represents the residual aberration expressed in percentage, calculated with or without the corresponding optimization factor.

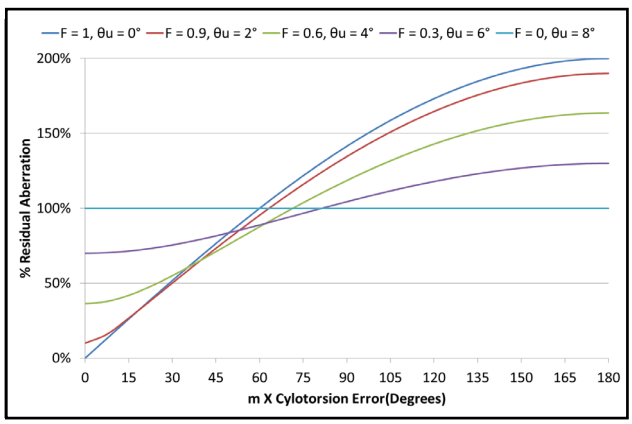

Figure 2. The percentage residual aberration (with the modal optimization) with increasing angular frequency *(m)* and cyclotorsion error for varying cyclotorsion measurement uncertainty. The X-axis being a product of angular frequency and cyclotorsion error represents the behaviour of the modal method (for different measurement uncertainties) for a range of angular frequencies in combination with a range of cyclotorsion error. The Y-axis represents the residual aberration (expressed in percentage) calculated for a veritable cyclotorsion error, however, using the modal optimization factor considering cyclotorsion measurement uncertainty.

by measurement uncertainty. Therefore, we must account for the performance of the method in case the cyclotorsion error is different from the one assumed a priori. In order to compare the performance of the modal method with and without an accurate cyclotorsion error measurement, we calculate the percentage residual aberration (using Eq.8) based on the optimization factor (Modal approach using Eq.13) calculated for a range of cyclotorsion uncertainty (θ_u) from 0° to 8°. This range was chosen to cover at least twice the typical mean expected value (~4°) of measurement uncertainty affecting the measured cyclotorsion error, as discussed below. Figure 2 demonstrates the performance of the modal method if the cyclotorsion error (affected by the measurement uncertainty) differs from the one assumed a priori for rotating an ablation profile during the refractive procedure. Here, θ_u is shown with the corresponding minimization factor value.

The quantity F = 0 (corresponding to θ_u = 8°) in Figure 2 represents the residual aberrations without any optimization for the cyclotorsion uncertainty. One can observe that for lower cyclotorsion uncertainties (θ_u = 2°), the gains in residual aberration for lower cyclotorsion error and angular frequencies are not substantial. However, the gains show their effect more as the angular frequency *(m)* and cyclotorsion error (θ) increase. On the other hand, for higher cyclotorsion uncertainties (θ_u = 4° and θ_u = 6°), losses are observed for lower angular frequencies and cyclotorsion errors, stabilizing at higher *m* and θ, and subsequently continue to improve. This is because of the dominant effect of the modal factor for higher cyclotorsion uncertainties. This implies that planning using the modal approach will impede the performance for some lower order terms but result in improvements while planning the higher order terms. The magnitude of these improvements will depend on the degree of uncertainty in cyclotorsion error measurement and the cyclotorsion error itself.

DISCUSSION

It is important to realize the extent of the effect of cyclotorsion on visual outcomes. This question was addressed in a previous paper[9], where we discussed the clinical effects of pure cyclotorsional errors during refractive surgery, assuming that the cyclotorsion measurement is accurate and not subject to any measurement errors. It is always preferable to prevent or measure and compensate the cyclotorsion error, but in any compensation there is always an inherent risk of failure resulting from uncertainties in measurement and compensation, leading to residual cyclotorsion. Furthermore, a risk of unsuccessful registration (i.e. no compensation) also exists. The currently-used laser systems are designed either with or without cyclotorsion control. Planning refractive surgery using the presented approaches will have implications in both cases.

If the system in use has cyclotorsion controls, then we can consider the cyclotorsion measurement uncertainty

affecting the procedure. Even with sophisticated measurement techniques, the assumption can never be made that cyclotorsion errors are measured perfectly and hence compensated perfectly with a corresponding rotated ablation profile. One can assume ~2° uncertainty due to the relative orientation between the eye-tracking camera and scanners (ANSI Z80.11-2012); this would translate to a further ~2° uncertainty due to the relative orientation between the Hartmann Shack (H-S) camera and the iris camera. Another ~2° uncertainty can be considered due to the registration algorithm[18]. All these factors together result in an RMS cyclotorsion measurement uncertainty of ~3.4° with peaks of up to at least 6° (2°+2°+2°). Based on the RMS cyclotorsion measurement uncertainty, a good starting point for such systems is to consider a typical mean expected value of about ~4° of measurement uncertainty affecting the measured cyclotorsion error. On the other hand, for laser systems without cyclotorsion compensation, an average value of ~3-4° of cyclotorsion errors with peaks of up to at least 14°[19] can be assumed to affect the refractive procedure.

For the modal approach, the difference in the optimized and non-optimized residual aberrations is non-linear and dramatically increases for larger cyclotorsion uncertainty or higher angular frequencies, as evident in Figures 1A and 1B. The minimization factor ranges from +1 to –1 (in percentage +100% to –100%). The effect of the modal minimization factor on laser systems without cyclotorsion control can be deduced from Figure 1A. An average cyclotorsion error of 4° would imply an improvement observed for radial orders higher than 7. However, for extreme cases of cyclotorsion (~12°), this improvement will start to present from the third radial order and higher. This conclusion is based on the improvements in percentage residual aberrations (Figure 1A) with modal optimization factor, starting to appear from *m* X cyclotorsion error ~30. More importantly, the use of this approach will never impede the performance in systems without cyclotorsion control. The performance gains, however, will be observed only in extreme cases of cyclotorsion movements.

The effect of the modal minimization factor on laser systems with cyclotorsion control can be deduced from Figure 2. Assuming an average measurement uncertainty of 2°[19], the progression of F = 0.9 (θ_u = 2°) in Figure 2 represents the behaviour of the modal approach for increasing angular frequency and cyclotorsion error. Comparing this to F = 1 (θ_u = 0°) for an average cyclotorsion error (θ) of 4° suggests that the modal approach will impede the performance marginally for third and lower radial orders. However, for fourth and higher radial orders, this method will improve the system performance, resulting in lower residual aberrations. Considering even higher cyclotorsion uncertainties, the losses are comparatively higher for lower angular frequencies and cyclotorsion errors, stabilize at higher *m* and θ and subsequently continue to improve. For evaluating the performance of this method, we can base our analysis on mean values of measurement uncertainties (~4°) and cyclotorsion errors (~4°). Owing to the impeding performance of this method for lower orders, one could explore a combination of two approaches for planning refractive surgery, where the lower order terms can be planned based on the conventional approach of rotated ablation profiles and higher order terms can be planned with optimized rotated ablation profiles based on the factor calculated through the modal approach. Furthermore, due to the independence seen in the clinics for planning the lower (zero to second order) and higher order (third order and higher) terms, the use of a combination of these approaches holds good potential.

As the calculated minimization factors are always <1, an "overplanned" treatment will never minimise the residual wavefront aberration, independent of the cyclotorsion uncertainty. Furthermore, an "underplanned" treatment calculated using the presented approach will not only minimise the residual aberration magnitude imposed by the higher order terms, but relatively orient the residual aberrations closer to the original aberration pattern.

We must acknowledge that the gains using the modal approach do not substantially improve the currently used methods. However, at such low implementation costs, any improvement could be worth exploring. In addition, we also evaluated a global minimization factor along similar lines; however, the gains while using the global minimization method were very modest, even at higher cyclotorsion uncertainties. For this reason we have excluded their presentation in this paper.

Shi et al.[14] developed an SPGD-based algorithm to optimize the wavefront-guided correction that improves visual acuity given cyclotorsion errors, based on measured scleral contact lens movements for three keratoconous eyes. They adopted a single value image quality metric highly correlated with the visual acuity, and did not use RMS wavefront error to predict visual performance. They found that partial magnitude corrections optimized with an SPGD algorithm led to improvements in visual acuity and compensated for cyclotorsion errors. In our theoretical approach, we followed a more mathematically-oriented method to minimize the component of residual aberration with a minimization factor. This minimization factor ranges between –1 to +1 and concurs with the results of Shi et al.[14] Furthermore, we also conclude in favour of underplanning treatment to reduce the negative impact of the cyclotorsion uncertainties. However, our analysis of the modal method suggests that it is suitable for improving the performance for only the higher order Zernike terms for laser systems equipped with cyclotorsion compensation controls. For the laser systems with no cyclotorsion compensation controls, the use of this method will only improve the performance. One can implement this approach without repeatedly measuring the eye movements, with

a simple nomogram adjustment based on the estimated cyclotorsion uncertainty and the Zernike mode.

We evaluated the performance of these methods based on the RMS of wavefront aberrations, theoretically regraded as a major metric to evaluate visual performance. The ease of implementation of these methods shall be weighed against the modest gains for evaluating their performance. In summary, special attention must be paid to intended or unintended overcorrections of the customised patterns. We can theoretically conclude that purposely underplanned treatments considering cyclotorsion uncertainties have more potential in restricting the effects of cylotorsion and reducing the residual wavefront aberrations imposed by the higher order Zernike terms.

REFERENCES

1. Zernike F. Beugungstheorie des schneidenver-fahrens und seiner verbesserten form, der phasenkontrastmethode. Physica. 1934; 1:689-704.
2. Huang D, Arif M. Spot size and quality of scanning laser correction of higher-order wavefront aberrations. J Cataract Refract Surg. 2002; 28:407-16.
3. Guirao A, Williams D, MacRae S. Effect of beam size on the expected benefit of customized laser refractive surgery. J Refract Surg. 2003; 19:15-23.
4. Bueeler M, Mrochen M. Simulation of eye-tracker latency, spot size, and ablation pulse depth on the correction of higher order wavefront aberrations with scanning spot laser systems. J Refract Surg. 2005; 21:28-36.
5. Bueeler M, Mrochen M, Seiler T. Effect of eye movements during refractive surgery with a scanning spot laser. Proceedings of the SPIE. 2003; 4951:150-60.
6. Porter J, Yoon G, MacRae S, et al. Surgeon offsets and dynamic eye movements in laser refractive surgery. J Cataract Refract Surg. 2005; 31:2058-66.
7. Smith EM Jr, Talamo JH. Cyclotorsion in the seated and the supine patient. J Cataract Refract Surg. 1995; 21:402-3.
8. Bueeler M, Mrochen M Seiler T. Maximum permissible lateral decentration in aberration-sensing and wavefront-guided corneal ablations. J Cataract Refract Surg. 2003; 29:257-63.
9. Arba Mosquera S, Merayo-Lloves J, de Ortueta D. Clinical effects of pure cyclotorsional errors during refractive surgery. Invest Ophthalmol Vis Sci. 2008; 49: 4828-36.
10. Aslanides IM, Toliou G, Padroni S, Arba Mosquera S, Kolli S. The effect of static cyclotorsion compensation on refractive and visual outcomes using the Schwind Amaris laser platform for the correction of high astigmatism. Cont Lens Anterior Eye. 2011; 34:114-20.
11. Arba Mosquera S, Arbelaez MC. Use of a six-dimensional eye-tracker in corneal laser refractive surgery with the SCHWIND AMARIS TotalTech Laser. J Refract Surg. 2011; 27:582-90.
12. Arba-Mosquera S, Arbelaez MC. Three-month clinical outcomes with static and dynamic cyclotorsion correction using the SCHWIND AMARIS. Cornea. 2011; 30:951-7.
13. Swami AU, Steinert RF, Osborne WE, White AA. Rotational malposition during laser in situ keratomileusis. Am J Ophthalmol 2002; 133:561-2.
14. Shi Y, Queener HM, Marsack JD, Ravikumar A, Bedell HE, Applegate RA. Optimizing wavefront-guided corrections for highly aberrated eyes in the presence of registration uncertainty. J Vis. 2013; 13:8.
15. Bará S, Arines J, Ares J, Prado P. Direct transformation of Zernike eye aberration coefficients between scaled, rotated, and/or displaced pupils. J Opt Soc Am A Opt Image Sci Vis. 2006; 23:2061-6.
16. Lundström L, Unsbo P. Transformation of Zernike coefficients: scaled, translated, and rotated wavefronts with circular and elliptical pupils. J Opt Soc Am A Opt Image Sci Vis. 2007; 24:569-77.
17. Guirao A, Williams DR, Cox IG. Effect of rotation and translation on the expected benefit of an ideal method to correct the eye's higher-order aberrations. J Opt Soc Am A Opt Image Sci Vis. 2001; 18:1003-15.
18. Chernyak DA. Cyclotorsional eye motion occurring between wavefront measurement and refractive surgery. J Cataract Refract Surg. 2004; 30:633-8.
19. Arba Mosquera S, Verma S. Effects of torsional movements in refractive procedures. J Cataract Refract Surg. 2015; 41:1752-66.

First author:

Samuel Arba Mosquera , PhD

SCHWIND eye-tech-solutions GmbH. Kleinostheim, Germany.